Field evolution of magnetic correlation lengths in ϵ-Co nanoparticle assemblies

M. Sachan,[1] C. Bonnoit,[1] S. A. Majetich,[1,a)] Y. Ijiri,[2] P. O. Mensah-Bonsu,[2] J. A. Borchers,[3] and J. J. Rhyne[4]
[1]*Physics Department, Carnegie Mellon University, Pittsburgh, Pennsylvania 15213, USA*
[2]*Department of Physics and Astronomy, Oberlin College, Oberlin, Ohio 44074, USA*
[3]*NIST Center for Neutron Research, National Institute of Standards and Technology, Gaithersburg, Maryland 20899, USA*
[4]*Los Alamos National Laboratory, Los Alamos, New Mexico 87545, USA*

(Received 28 January 2008; accepted 28 March 2008; published online 15 April 2008)

Small-angle neutron scattering measurements of Co nanoparticle assemblies reveal three characteristic length scales associated with the interparticle and intraparticle magnetic orders. The first length scale stemming from particle size and separation does not vary with applied field. In contrast, the magnetic correlation length increases from 71 ± 9 nm in zero field at 5 K to greater than 1000 nm in fields larger than 0.2 T. The random-field length scale decreases from 37 ± 8 nm when $H=0$ to 9.1 ± 0.3 nm in $H=0.2$ T, and the contribution of this term is less significant in large fields. © *2008 American Institute of Physics*. [DOI: 10.1063/1.2911736]

Magnetic correlations between nanoscale grains can affect the performance of hard disk recording media, where nonuniformity is a source of noise that can limit the minimum bit size. In clusters of nanoparticles proposed for hyperthermic cancer treatment,[1] the optimal operating frequency may depend on the magnetic correlation length.[2] Due to the uniformity in their size and spacing, surfactant-coated single domain nanoparticle arrays are an excellent system for testing models of magnetic correlations.[3,4] The determination of correlation lengths in these arrays will help to develop quantitative analytic techniques for more complex but technologically important magnetic nanostructures.

Here, we report a comprehensive approach in understanding the collective behavior of magnetic nanoparticle assemblies, using small-angle neutron scattering (SANS). While previous SANS experiments have probed nanoscale correlation lengths,[5–13] SANS has only more recently been applied to dense arrays of surfactant-coated nanoparticles.[14–16] The high degree of uniformity in our nanoparticle crystals leads to a pronounced diffraction peak and allows for a straightforward interpretation of interparticle and intraparticle interaction lengths.

Surfactant-coated 7.9 ± 1.3 nm ϵ-Co nanoparticles (Fig. 1) were synthesized by high temperature air-free solution phase methods,[17] and then used to self-assemble fcc nanoparticle three-dimensional (3D) crystals, as described elsewhere.[18] The average edge-to-edge spacing was 4.2 ± 1.0 nm so exchange interactions were negligible. The native oxide shell thickness was estimated using magnetometry, atomic absorption spectroscopy, and transmission electron microscopy (TEM) to determine saturation moment, total Co concentration, and average particle diameter, respectively. Assuming uniform core-shell particles with completely aligned Co core spins of bulk saturation magnetization and antiferromagnetic CoO shells with no net moment, the average shell thickness was then estimated to be 0.75 ± 0.4 nm. With these particles, there was no detected shift in the field-cooled hysteresis loop due to exchange bias. The zero field-cooled magnetization showed a sharp rise near 90 K, and then a broad peak that had only slightly decayed at 300 K.

For the SANS measurements, dried powders of the Co nanoparticle crystals were prepared in argon and then sealed in an Al container that was inserted into a 7 T horizontal field superconducting magnet. The neutron experiments were performed on the NG7 SANS beam line at NIST using 0.5 nm wavelength λ neutrons in transmission and a two-dimensional position sensitive detector. Two different detector distances were used to cover the scattering vector $Q=4\pi \sin \theta/\lambda$ range from 0.04 to 1.0 nm^{-1}. A magnetic field was applied perpendicular to the neutron beam and in the plane of the sample.

Figure 2 maps the scattering intensity I with and without an applied magnetic field H as a function of scattering vector components Q_x and Q_y. Note that both chemical and magnetic structures contribute, although only the magnetic scattering varies with H. In $H=0$, the intensity is symmetric, pronounced at low Q, and displays a diffraction ring at a Q position determined by the particle spacing. When a 5 T nearly saturating field is applied in the x direction, the overall intensity drops because the magnetic scattering at low Q collapses to $Q=0$ as the moments align. Since only the magnetization component perpendicular to Q contributes to the

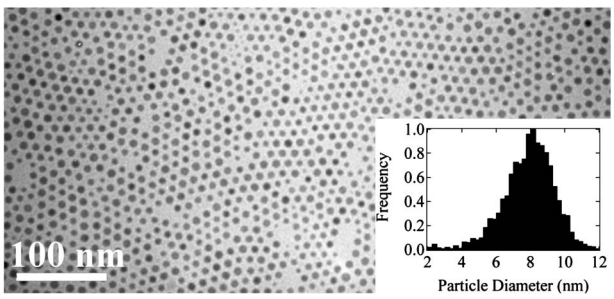

FIG. 1. TEM image of 7.9 ± 1.3 nm nanoparticles (inset: particle size distribution). SANS sample is a 3D nanoparticle crystal with longer-range structural order.

a)Electronic mail: sara@cmu.edu.

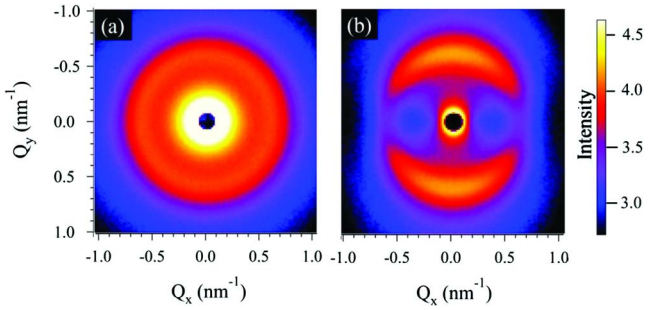

FIG. 2. (Color online) Two-dimensional $I(Q)$ at 5 K (a) at 0 T and (b) 5 T applied along x. Note the asymmetry at 5 T.

scattering, $I \propto \sin^2 \alpha$ at the diffraction peak and in the low Q regions, where α is the angle between Q and H. Note the moments in the antiferromagnetic oxide shell of the Co particles contribute little to the scattering, in contrast to our previous work on Fe particles.[15]

To isolate the nuclear scattering, we performed a sector average ($\pm 5°$) of the intensity at $\alpha=0°$ for 5 T, where there would be minimal magnetic scattering. Here, we focus on the scattering at $\alpha=90°$ where the magnetic contribution to the intensity is greatest. In particular, we investigate $I_{\mathrm{mag}}(Q,H,90°)=I(Q,H,90°)-I(Q,5\ \mathrm{T},0°)$. Figure 3 depicts this magnetic signal as a function of Q for different applied fields.

$I_{\mathrm{mag}}(Q)$ reveals two major features: a Bragg diffraction peak due to the arrays of particle moments that is fit with a Gaussian function (G), and low Q scattering due to different correlation lengths that is fit with the sum of a Lorentzian squared (S) and a Lorentzian function (L)

$$I_{\mathrm{mag}} = N_G e^{-(Q-Q_G)^2/2\sigma_G^2} + \frac{N_S}{(\kappa_S^2+Q^2)^2} + \frac{N_L}{(\kappa_L^2+Q^2)}. \qquad (1)$$

Coherent scattering from a point lattice theoretically has a S lineshape at low Q, plus a higher Q decay that is inversely proportional to Q^2 and can be approximated by a L term.[19] All three terms are needed for reasonable fits, as shown in Fig. 3, with parameters in Table I.

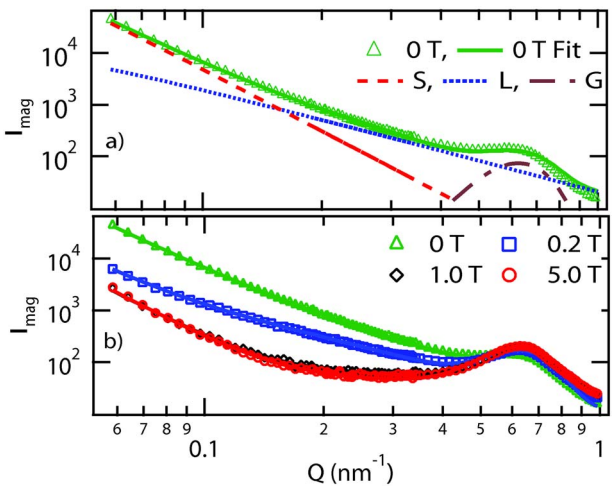

FIG. 3. (Color online) Background-subtracted $I_{\mathrm{mag}}(Q)$ versus Q at 5 K (a) for 0 T, showing the contributions from the S Lorentzian squared, L Lorentzian, and G Gaussian terms in Eq. (1). (b) Data and fits for different magnetic fields.

TABLE I. Fitting parameters as a function of field. $\xi_L=1/\kappa_L$; $\xi_S=1/\kappa_S$, where κ_L, κ_S, N_L, N_S, and N_G are as defined in Eq. (1). $Q_G=0.629\ \mathrm{nm}^{-1}$ and $\sigma_G=0.109\ \mathrm{nm}^{-1}$ for all H.

	0 T	0.2 T	1.0 T	5.0 T
ξ_L	37 ± 8	9.1 ± 0.3	1.4 ± 0.1	0.9 ± 0.2
ξ_S	72 ± 9	91 ± 14	1000	1000
N_L	20.55 ± 0.15	14.2 ± 0.4	33 ± 3	54 ± 18
N_S	0.490 ± 0.004	0.067 ± 0.002	0.0276 ± 0.0003	0.0278 ± 0.0003
N_G	62 ± 3	109 ± 3	130 ± 3	132 ± 3

The G term describes Bragg scattering at a d-spacing characteristic of the (111) separation of a fcc lattice of nanoparticles.[16,20] Using the average surfactant thickness and the core size distribution found from TEM, the center of the G peak in the SANS data ($0.629\ \mathrm{nm}^{-1}$) matches well to the TEM value of $0.632\ \mathrm{nm}^{-1}$. These results suggest that the nanoparticles are crystalline and not glassy.[15] The estimated full width at half maximum for the Gaussian peak (based on variances in neutron wavelength and the TEM particle size and spacing) is within 20% of the $0.26\ \mathrm{nm}^{-1}$ value extracted from the data fit.

While the diffraction peak originates from the nanoparticle lattice periodicity, long-range interparticle magnetic correlations generate scattering at lower Q. As the applied field increases, the overall intensity at low Q drops as magnetic regions align parallel to the field, resulting in changes in the magnetic length scales. A S dependence is the Fourier transform of a spatial correlation function of particle moments, $\langle \mu(0)\mu(r)\rangle \propto \exp(-\kappa_S r)$, with a characteristic decay length $\xi_S=1/\kappa_S$. It has frequently been observed in ferromagnets and is often associated with static magnetic correlations.[6,7] At 5 K and zero field, ξ_S is 71 ± 9 nm, which is much larger than the size of a single particle. It increases to 1000 nm or more in 1.0 T. Since SANS is sensitive to length scales $\leqslant$1000 nm, this value is indistinguishable from an infinite correlation length. The field variation of the magnetic correlation length indicates small domainlike regions with uniform magnetization even in zero field, with increasing domain size as H rises.

A $S+L$ intensity has been reported in numerous materials with random internal fields,[6,7,21] and a magnetic nanoparticle array would be expected to have inhomogeneous local fields unless fully saturated. A L dependence is the Fourier transform of a correlational function $\langle \mu(0)\mu(r)\rangle \propto [\exp(-\kappa_L r)]/r$, with a characteristic decay length of $\xi_L=1/\kappa_L$. ξ_L is 37 ± 8 nm when $H=0$ at 5 K, indicating magnetic inhomogeneities of a few particle diameters' length. As the field increases, ξ_L drops to $\sim$1 nm, corresponding to misaligned groups of spins within a particle (Table I).

The fitting parameters also indicate the relative amounts of scattering from the different terms. For comparison, analysis of the nuclear scattering using Eq. (1) yields $\xi_S \sim 1000$ nm and $\xi_L \sim 2$ nm. The $H=0$ magnetic ξ_S length is thus limited not by positional order but more likely by variations in magnetostatic coupling strengths due to crystallographic misorientations or small spacing differences. As the field increases, the total intensity of the S term arising from the domainlike regions becomes more prominent, while the L term that is associated with inhomogeneities decreases. These results suggest that the overall alignment increases and saturates above 1.0 T, consistent with hysteresis loops

measurements at 10 K, which indicate a magnetization to saturation magnetization ratio of 0.6 at 0.2 T but nearly 1.0 by 1.0 T.

Compared to other SANS studies of nanomagnets, our results show significant features which warrant a different interpretation, with a S function to describe the length scale of the multiparticle correlations plus a L term due to local inhomogeneities. Previously, scattering from assemblies of 2 nm Fe nanoparticles in an alumina matrix was modeled in terms of a S function for the particle cores, *multiplied* by a function with a L factor associated with multiparticle correlations.[8] The resultant length scales were shorter and consistent with the small particle size. SANS experiments on compacted[9] and electrodeposited[5] nanocrystalline solids have also revealed magnetic inhomogeneities. In the latter work, the correlation length described the length scale of the misaligned regions, which decreased as the applied field increased.[5] While this is similar to the drop seen here in ξ_L associated with misaligned spins, our nanoparticles are hard to saturate, and the length scale ξ_S associated with the regions of uniformly aligned particles remains small enough to be detected by SANS at low fields. The observed 70 nm magnetic correlational length in zero field thus serves as a benchmark for future work with related surfactant-separated nanoparticles.

We have demonstrated the existence of multiparticle magnetic correlations in 3D nanoparticle assemblies, even in the absence of an applied field. The intrinsic particle monodispersity and the uniformity of the particle separation allows for quantitative fitting of the results using a simple model that provides an intuitive understanding of the magnetization process. Length scales associated with multiparticle "domains," magnetic homogeneity, and periodic packing of the nanoparticles are extracted. As the field increases, the domain size increases while the magnetic disorder diminishes.

S.A.M. acknowledges the support from NSF Grant Nos. ECS-0304453 and ECS-0507050. Y.I. acknowledges the support from the ACS-PRF Grant No. 40049-B5M and Research Corporation Grant No. CC5820. This work utilized facilities supported in part by the NSF under Agreement No. DMR-0454672. We are grateful to J. G. Barker, J. Krzywon, and B. Greenwald for their scientific assistance with SANS, and to J. Weissmüller for helpful discussions.

[1] Q. A. Pankhurst, J. Connolly, S. K. Jones, and J. Dobson, J. Phys. D **36**, R167 (2003).
[2] A. Eggemann, S. A. Majetich, D. F. Farrell, and Q. Pankhurst, IEEE Trans. Magn. **43**, 2451 (2007).
[3] S. A. Majetich and M. Sachan, J. Phys. D **39**, R407 (2006).
[4] D. F. Farrell, Y. Cheng, R. W. McCallum, and S. A. Majetich, J. Phys. Chem. B **109**, 13409 (2005).
[5] A. Michels, R. N. Viswanath, J. G. Barker, R. Birringer, and J. Weissmüller, Phys. Rev. Lett. **91**, 267204 (2003).
[6] G. Grinstein and D. Mukamel, Phys. Rev. B **27**, 4503 (1983).
[7] R. L. Leheny, Y. S. Lee, G. Shirane, and R. J. Birgeneau, Eur. Phys. J. B **32**, 287 (2003).
[8] C. Bellouard, I. Mirebeau, and M. Hennion, Phys. Rev. B **53**, 5570 (1996).
[9] J. F. Löffler, H. B. Braun, and W. Wagner, Phys. Rev. Lett. **85**, 1990 (2000).
[10] A. Wiedenmann, Physica B **297**, 226 (2001).
[11] J. R. Childress, C. L. Chien, J. J. Rhyne, and R. W. Erwin, J. Magn. Magn. Mater. **104-107**, 1585 (1992).
[12] T. Oku, E. Ohta, T. Sato, M. Furusaka, M. Imai, and Y. Matsushita, J. Magn. Magn. Mater. **188**, 291 (1998).
[13] F. Carsughi, G. Baio, D. Rinaldi, T. Guidi, R. Caciuffo, and D. Fiorani, J. Magn. Magn. Mater. **272-276**, e1173 (2004).
[14] T. Thomson, S. L. Lee, M. F. Toney, C. D. Dewhurst, F. Y. Ogrin, C. J. Oates, and S. Sun, Phys. Rev. B **72**, 064441 (2005).
[15] Y. Ijiri, C. V. Kelly, J. A. Borchers, J. J. Rhyne, D. F. Farrell, and S. A. Majetich, Appl. Phys. Lett. **86**, 243102 (2005).
[16] D. F. Farrell, Y. Ijiri, C. V. Kelly, J. A. Borchers, J. J. Rhyne, Y. Ding, and S. A. Majetich, J. Magn. Magn. Mater. **303**, 318 (2006).
[17] V. F. Puntes, D. Zanchet, C. K. Erdonmez, and A. P. Alivisatos, J. Am. Chem. Soc. **124**, 12874 (2002).
[18] M. Sachan, N. D. Walrath, S. A. Majetich, K. Krycka, and C. C. Kao, J. Appl. Phys. **99**, 08C302 (2006).
[19] N. Bernhoeft, Acta Crystallogr., Sect. A: Found. Crystallogr. **55**, 274 (1999).
[20] D. F. Farrell, Y. Cheng, S. Kan, M. Sachan, Y. Ding, and S. A. Majetich, J. Phys.: Conf. Ser. **17**, 185 (2005).
[21] S. B. Dierker and P. Wiltzius, Phys. Rev. Lett. **66**, 1185 (1991).